Published in final edited form as:
J Am Chem Soc. 2020 February 26; 142(8): 4061–4069. doi:10.1021/jacs.0c00335.

Stereospecific Furanosylations Catalyzed by Bis-Thiourea Hydrogen-Bond Donors

Andrew B. Mayfield[‡,†], **Jan B. Metternich**[‡], **Adam H. Trotta**, **Eric N. Jacobsen**[*]
Department of Chemistry & Chemical Biology, Harvard University, Cambridge, Massachusetts 02138, United States

Abstract

We report a new method for stereoselective *O*-furanosylation reactions promoted by a precisely tailored bis-thiourea hydrogen-bond-donor catalyst. Furanosyl donors outfitted with an anomeric dialkylphosphate leaving group undergo substitution with high anomeric selectivity, providing access to the challenging 1,2-*cis* substitution pattern with a range of alcohol acceptors. A variety of stereochemically distinct, benzyl-protected glycosyl donors were engaged successfully as substrates. Mechanistic studies support a stereospecific mechanism in which rate-determining substitution occurs from a catalyst–donor resting-state complex.

Graphical Abstract

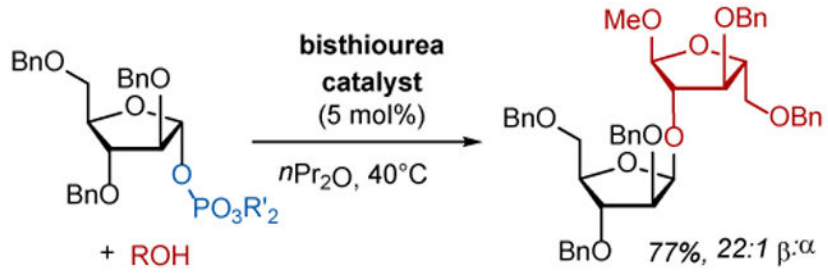

INTRODUCTION

Oligo- and polyfuranosides, although less prevalent than corresponding pyranose-based saccharides, are distributed broadly in mammals, plants, and bacteria.[1-4] Furanosides bearing 1,2-*cis*-*O*-glycosidic linkages are found in many biologically important oligosaccharides, such as the complex cell-wall polysaccharide rhamnogalacturonan II,[5-7] the cellular marker poly-(ADP)ribose involved in DNA repair and apoptosis,[8,9] and the cell-

[*]Corresponding Author jacobsen@chemistry.harvard.edu.
[†]**Present Addresses** Department of Chemistry, Stanford University, Stanford, California 94305, United States
[‡]**Author Contributions** These authors contributed equally.

The authors declare no competing financial interests

The Supporting Information
The Supporting Information is available free of charge on the ACS Publications website at DOI: https://pubs.acs.org/doi/10.1021/jacs.0c00335
Experimental Procedures and characterization data
Crystallographic data for **3r**

wall constituent arabinogalactan found in mycobacteria.[10-14] These 1,2-*cis*-linkages present significant synthetic challenges, some common to any glycosylation, and others intrinsic to furanosylations. Traditional anchimeric assistance approaches produce 1,2-*trans*-glycosides, and are generally not applicable to 1,2-*cis*-glycosylation.[15,16] The conformational and electronic properties of furanoses render them more prone than pyranoses to S_N1 pathways, [17] and while deep insight has been gleaned into the factors controlling facial selectivity in additions to the intermediate cyclic oxocarbenium ions, no general solutions exist.[18-21] Approaches relying on stereospecific substitution of an anomerically pure donor are rendered difficult by the faster anomerization rate for furanoses relative to pyranoses.[22-26] Taken together, these considerations imply that many of the methods developed for selective pyranosylations will not translate readily to furanosylations, especially those that rely on substrate control.

Motivated by the importance of the targets and the fundamental challenges outlined above, several research groups have developed elegant strategies for the construction of 1,2-*cis*-*O*-furanoses, including intramolecular aglycone delivery,[27-29] conformationally-locked oxocarbenium formation,[30-35] and selective opening of 2,3-anhydro sugars,[36] among others. [37-49] These strategies are highly effective in specific cases, but they each rely on specialized protecting and/or directing groups on the glycosyl donor, thereby limiting their generality.

Inspired by enzymatic glycosylations that proceed via stereospecific displacement of phosphate leaving groups,[50-62] our group recently discovered that bis-thiourea hydrogen-bond donors such as **4a** (Figure 2) catalyze the stereospecific addition of alcohol acceptors to pyranosyl phosphate donors (Figure 1B).[63] The catalysts are hypothesized to engage the anomeric phosphate leaving group through a network of hydrogen bonds, while activating the acceptor through a general base interaction with one of the amides on the catalyst. With the goal of developing general protocols for 1,2-*cis*-furanosylation reactions, we envisioned extending this strategy to furanose substrates through the discovery of an appropriate phosphate leaving group and complementary hydrogen-bond-donor catalyst.

RESULTS AND DISCUSSION

The coupling of arabinofuranosyl phosphates **1** and galactose bis-acetonide **2a** was investigated as a model reaction (Figure 2).[64] Proper selection of the phosphate leaving group proved critical: diarylphosphates (e.g. **1a**)[65-68] were too unstable to allow isolation, whereas acyclic dialkylphosphates (e.g. **1b**)[69-71] were poorly reactive in the presence of bis-thiourea **4a**. In contrast, the cyclic phosphate donor **1c** underwent substitution with increased reaction rates.[72,73] We observed nearly complete inversion at the anomeric center, providing initial evidence for a catalyst-promoted stereospecific pathway. As previously observed in related hydrogen-bond-donor catalyzed glycosylations of pyranosyl phosphates, the use of ethereal solvents and inclusion of molecular sieves in the reaction medium proved critical.[63] We hypothesize that the sieves mitigate unproductive hydrolysis of the donor, and sequester the phosphoric acid byproduct, which could exert a detrimental effect on anomeric selectivity.

Bis-thiourea catalysts closely related to **4a** were found to be uniquely effective in catalyzing the model furanosylation with good reaction rates and stereospecificity, prompting catalyst optimization through subtle variations to this dimeric scaffold (Table 1).[74,75] We selected threonine derivative **2b** as a relatively challenging model secondary alcohol acceptor during catalyst optimization. We found that reactions employing **2b** furnished the desired furanoside **3b** more slowly than reactions conducted with primary alcohol acceptor **2a**, but the β-selectivities remained comparable. Product yield could be used as an approximate gauge of reaction rate since the reactions were found to be clean and well-behaved, with no evidence of catalyst deactivation and continued conversion beyond the standard 18 h reaction time. Conducting the model reaction with the enantiomeric catalyst *ent*-**4a** resulted in a slightly lower reaction rate and a significantly lower β-selectivity, which is consistent with a match/mismatch effect with the donor and/or the acceptor. Other modifications—addition of methyl substituents on both arylpyrrolidines (**4b**), epimerization of the aryl substituent on the bottom pyrrolidine (**4c**), or removal of one carbon from the linker (**4d**)—failed to generate catalysts that improved both yield and β-selectivity. However, we observed improved reaction rates with catalysts lacking substitution on the bottom pyrrolidine (**4e**–**4g**), which was coupled with excellent β-selectivity when the top arylpyrrolidine was also outfitted with a methyl substituent (**4f**).

Additional improvements to catalytic efficiency could be achieved through modification of the aryl group on the top pyrrolidine (Table 2A). Generally, expanded 2-aryl substituents improved both stereoselectivity and conversion, leading to the identification of the 2-naphthyl derivative **4i** as the optimal catalyst. A series of control experiments were conducted, highlighting important structural features of the optimal catalyst and revealing the unique ability of this precisely linked bis-thiourea scaffold to catalyze the furanosylation in high yield and β-selectivity (**4l**, *ent*-**4i**, and **4m**, Table 2).

The scope of acceptors in the arabinosylation reaction using phosphate ester **1c** and catalyst **4i** was examined (Table 3) Reactions were carried out using 2 equiv. of the acceptor, although only slightly diminished rates and comparable b selectivities were also obtained with lower ratios (Tables S3, S4, and Figures S16, S18). A variety of glycosyl acceptors participate effectively in the catalytic reaction, yielding the desired 1,2-*cis* products with high stereoselectivities and generally good yields (Table 1). For example, both primary and secondary pyranose- and furanose-derived acceptors with differing stereochemical patterns undergo reaction to afford the β-glycosides selectively. In this manner, the biologically important β-arabinose (1→2) arabinose linkage could be constructed using the C2-hydroxy arabinofuranose acceptor **2o**.[10-14] Primary and secondary alcohol-containing carbamate-protected amino esters were also effective substrates. The reaction conditions proved to be compatible with a variety of protecting groups, including benzylidene acetals (**2h**), acetonides (**2a**, **2e**–**2g**), and *tert*-butyl carbamates (**2b**, **2p**–**2r**), providing access to the β-arabinose-4-hydroxyproline glycoside **3r** found in cell-wall glycoproteins (see also Figure 3).[76-81] In nearly all cases examined, significant increases in β selectivity were observed under the optimized catalytic conditions when compared to the standard TMSOTf activation protocol (Table 3).[82] Some limitations to the methodology were identified nonetheless. For example, all mannose-derived acceptors examined were found to be unreactive. Coupling

with 1-*O*-methyl-2,3,4-tri-*O*-acetyl-α-D-glucose afforded product in high yield (~95%), but only moderate selectivity favoring the α-anomer (α:β 2.5:1). In that case, the uncatalyzed reaction afforded only α product and proceeded at a rate comparable that of the catalyzed reaction (Scheme S6).

The scope of the catalytic furanosylation protocol was evaluated with respect to the glycosyl donor using acetonide-protected 6-hydroxy galactopyranose **2a** (6-gal) as a representative acceptor (Table 4). Sugars harboring the same stereochemical pattern as arabinose performed well in the catalytic reaction (see Table 4A, **5a**–**5c**). Closely related fucofuranosyl[83,84] and galactofuranosyl[85,86] phosphate derivatives **5a** and **5b** underwent reaction to the desired disaccharides (**6a** and **6b**) in excellent yield and with good β-selectivity, demonstrating tolerance for variation of the C5-substituent. A C2-fluoro analog of arabinose **5c** displayed lower reactivity, although glycosylation could be accomplished in good yield and only slightly diminished anomeric selectivity by increasing reaction time and temperature (**6c**).[87-89]

Furanose derivatives stereoisomeric to D-arabinose were also employed as glycosyl donors (Table 2). Using the enantiomeric catalyst *ent*-**4i**, L-arabinose was found to react in a similar fashion to D-arabinose to yield **6d**, with the slightly different outcomes ascribable to the stereochemistry of the acceptor. Ribose—the C2 epimer of arabinose—was prepared as the β-phosphate donor **5e** and found to undergo invertive displacement to form the 1,2-*cis*-configured α-glycoside product **6e** in the presence of *ent*-**4i**. Lyxofuranose phosphate—the C3 epimer of arabinofuranose—was primarily isolated as the α-phosphate glycosyl donor (1:3 β:α), and was completely unreactive with either enantiomer of catalyst (data not shown). Xylofuranose phosphate **5f**—epimeric at both C2 and C3 relative to arabinose—was primarily isolated as the β-phosphate glycosyl donor (20:1 β:α).[83] However, unlike all of the other donors examined, it underwent reaction with net retention of configuration to form the β-configured disaccharide product **6f**.

To probe the stereospecific nature of the developed protocol, the effect of the donor anomeric composition on the reaction outcome was tested using arabinofuranose phosphate **1c**, ribose phosphate **5e**, and xylofuranose phosphate **5f**. For arabinose and ribose, decreasing the anomeric purity of the donor led to a decrease in reaction selectivity, providing evidence for a dominant stereospecific pathway (Table 5). These reactions are not perfectly stereospecific, which may be ascribed to donor epimerization (see below). In contrast, the anomeric purity of the xylofuranose phosphate donor **5f** had no effect on the selectivity of the reaction; we have not yet elucidated the unique mechanistic characteristics of that particular substrate.

Kinetic experiments were performed using 6-gal **2a** and *N*-Boc-L-threonine methyl ester **2b** as acceptors and arabinose phosphate **1c** as the donor. Examination of the time course data revealed that epimerization of the arabinose phosphate donor occurs slowly and in competition with the desired substitution reaction (Figures 4, S2-S6 and Tables S6-S14).[23-25] Slight deterioration of product anomeric selectivity was observed as the reaction progressed, consistent with glycosylation proceeding via an invertive mechanism from either anomer of the phosphate donor. Conversely, when using xylofuranose phosphate as the

donor, the reaction proceeded with increasing product anomeric selectivity and a concomitant decrease of donor anomeric purity (Figure S21-S22 and Tables S42-S44), suggesting that the unexpected retentive substitution outcome may be ascribed to selective reaction of the less-stable α-anomer.[90]

Kinetic analysis of the arabinosylation reaction revealed that both the glycosylation and the epimerization pathways are accelerated by the bis-thiourea catalyst (Figures S9-S10 and S16-S20, and Tables S21-S26). In contrast, the concentration of the acceptor affected the rate of glycosylation but not the rate of epimerization, consistent with rate-determining substitution catalyzed by the bis-thiourea hydrogen-bond donor through a stereospecific S_N2-like pathway. The rate of glycosylation was significantly less sensitive to the arabinosyl phosphate donor concentration relative to acceptor and catalyst concentration, but accurate determination of the kinetic order in donor was not possible due to its low solubility in ethereal solvents. However, the existence of a resting-state catalyst–donor complex under catalytic conditions was confirmed through ^{31}P NMR binding studies (Figures S23-S26).[91]

The epimerization pathway was found to be dependent on the concentration of the arabinosyl phosphate donor and could also be promoted by the phosphoric acid byproduct. The latter effect was studied in kinetic experiments carried out in the absence of molecular sieves; phosphoric acid **9** formation was monitored (Figure S27-S30), with competitive binding to the bis-thiourea catalyst observed by ^{31}P NMR. Decreases in the rate of glycosylation and in the anomeric purity of both the donor and the disaccharide product are observed in reactions carried out in the absence of molecular sieves, along with undesired hydrolysis product. Consequently, the molecular sieves are proposed to sequester adventitious water and the phosphoric acid byproduct, thus enhancing reaction rate, yield, and stereoselectivity.

A catalytic cycle that accounts for the experimental observations is provided in Scheme 1. We propose that a resting-state bis-thiourea–glycosyl phosphate complex **I-7** undergoes stereospecific and rate-limiting substitution in competition with an epimerization pathway promoted by the catalyst and an additional phosphate source (phosphoric acid **9** or substrate **1c**). The epimerization pathway is minimized through the addition of molecular sieves, which sequester the phosphoric acid byproduct efficiently.

CONCLUSION

In conclusion, a furanosylation reaction catalyzed by precisely designed bis-thiourea organocatalysts was developed. Substitution of an arabinosyl phosphate derivative with a variety of primary and secondary alcohol acceptors affords 1,2-*cis*-linked products selectively and in high yields. The methodology was extended successfully to other furanose donors bearing different substitution and stereochemical patterns. Kinetic experiments and ground-state binding studies are consistent with rate-determining stereospecific substitution of the furanosyl-phosphate donors by alcohol acceptors. Continuing efforts seek to extend the new methodology to other classes of non-hydroxylic nucleophiles.

Supplementary Material

Refer to Web version on PubMed Central for supplementary material.

ACKNOWLEDGMENT

This work was supported by the NIH through the Common Fund Glycoscience Program (U01 GM116249) and through GM116249 and GM43214, by the Alexander von Humboldt Foundation (Feodor Lynen Research Fellowship to J.B.M) and an NIH F32 Ruth L. Kirschstein National Research Service Award to A.H.T (GM126636). We thank Dr. Shao-Liang Zheng (Harvard University) for determination of the X-ray crystal structure.

REFERENCES

(1). Lindberg B Components of Bacterial Polysaccharides. Adv. Carbohydr. Chem. Biochem 1990, 48, 279–318. [PubMed: 2077871]

(2). Brennan PJ; Nikaido H The Envelope of Mycobacteria. Annu. Rev. Biochem 1995, 64, 29–63. [PubMed: 7574484]

(3). Lowary TL Synthesis and Conformational Analysis of Arabinofuranosides, Galactofuranosides and Fructofuranosides. Curr. Opin. Chem. Biol 2003, 7, 749–756. [PubMed: 14644185]

(4). Lowary TL Twenty Years of Mycobacterial Glycans: Furanosides and Beyond. Acc. Chem. Res 2016, 49, 1379–1388. [PubMed: 27294709]

(5). Mazeau K; Pérez S The Preferred Conformations of the Four Oligomeric Fragments of Rhamnogalacturonan II. Carbohydr. Res 1998, 311, 203–217. [PubMed: 9825523]

(6). Perez S; Rodriguez-Carvajal MA; Doco T A Complex Plant Cell Wall II. A Structure in Quest of a Function. Biochimie 2003, 85, 109–121. [PubMed: 12765781]

(7). Matsunaga T; Ishii T; Matsumoto S; Higuchi M; Darvill A; Albersheim P; O'Neill MA Occurrence of the Primary Cell Wall Polysaccharide Rhamnogalacturonan II in Pteridophytes, Lycophytes, and Bryophytes. Implications for the Evolution of Vascular Plants. Plant Physiol. 2004, 134, 339–351. [PubMed: 14671014]

(8). Morales JC; Li L; Fattah FJ; Dong Y; Bey EA; Patel M; Gao J; Boothman DA Review of Poly (ADP-ribose) Polymerase (PARP) Mechanisms of Action and Rationale for Targeting in Cancer and Other Diseases. Crit. Rev. Eukaryot. Gene Expr 2014, 24, 15–28. [PubMed: 24579667]

(9). Leung AKL Poly(ADP-ribose): An Organizer of Cellular Architecture. J. Cell Biol 2014, 205, 613–619. [PubMed: 24914234]

(10). Clarke AE; Anderson RL; Stone BA Form and Function of Arabinogalactans and Arabinogalactan-Proteins. Phytochem. 1979, 18, 521–540.

(11). Sharon N; Lis H Comparative Biochemistry of Plant Glycoproteins. Biochem. Soc. Trans 1979, 7, 783–799. [PubMed: 383552]

(12). Dey PM; Brinson K Plant Cell-walls. Adv. Carbohydr. Chem. Biochem 1984, 42, 265–382.

(13). Crick DC; Mahapatra S; Brennan PJ Biosynthesis of the Arabinogalactan-peptidoglycan Complex of Mycobacterium Tuberculosis. Glycobiology 2001, 11, 107R–118R.

(14). Tanner W Glykoproteine: Struktur, Biosynthese, Funktion. Ber. Deutsch. Bot. Ges. Bd 1986, 99, 237–249.

(15). Nigudkar SS; Demchenko AV Stereocontrolled 1,2-*cis* Glycosylation as the Driving Force of Progress in Synthetic Carbohydrate Chemistry. Chem. Sci 2015, 6, 2687–2704. [PubMed: 26078847]

(16). Mensink RA; Boltje TJ Advances in Stereoselective 1,2-*cis* Glycosylation Using C-2 Auxiliaries. Chem. Eur. J 2017, 23, 17637–17653. [PubMed: 28741787]

(17). Adero PO; Amarasekara H; Wen P; Bohé L; Crich D The Experimental Evidence in Support of Glycosylation Mechanisms at the S_N1–S_N2 Interface. Chem. Rev 2018, 118, 8242–8284. [PubMed: 29846062]

(18). Larsen CH; Ridgway BH; Shaw JT; Woerpel KA A Stereoelectronic Model to Explain the Highly Stereoselective Reactions of Nucleophiles with Five-Membered-Ring Oxocarbenium Ions. J. Am. Chem. Soc 1999, 121, 12208–12209.

(19). Larsen CH; Ridgway BH; Shaw JT; Smith DM; Woerpel KA Stereoselective C-Glycosylation Reactions of Ribose Derivatives: Electronic Effects of Five-Membered Ring Oxocarbenium Ions. J. Am. Chem. Soc 2005, 127, 10879–10884. [PubMed: 16076193]

(20). Rhoad JS; Cagg BA; Carver PW Scanning the Potential Energy Surface of Furanosyl Oxocarbenium Ions: Models for Reactive Intermediates in Glycosylation Reactions. J. Phys. Chem. A 2010, 114, 5180–5186. [PubMed: 20353189]

(21). Rijssel ER; van Delft P; Lodder G; Overkleeft HS; van der Marel GA; Filippov DV; Codée JDC Furanosyl Oxocarbenium Ion Stability and Stereoselectivity. Angew. Chem. Int. Ed 2014, 53, 10381–10385.

(22). Capon B Mechanism in Carbohydrate Chemistry. Chem. Rev 1969, 69, 407–498.

(23). Schray KJ; Benkovic SJ Anomerization Rates and Enzyme Specificity for Biologically Important Sugars and Sugar Phosphates. Acc. Chem. Res 1978, 11, 136–141.

(24). Pierce J; Serianni AS; Barker R Anomerization of Furanose Sugars and Sugar Phosphates. J. Am. Chem. Soc 1985, 107, 2448–2456.

(25). Prévost M; St-Jean O; Guindon Y, Synthesis of 1′,2′-*cis*-Nucleoside Analogues: Evidence of Stereoelectronic Control for SN2 Reactions at the Anomeric Center of Furanosides. J. Am. Chem. Soc 2010, 132, 12433–12439. [PubMed: 20704290]

(26). van der Vorm S; Hansen T; van Rijssel ER; Dekkers R; Madern JM; Overkleeft HS; Filippov DV; van der Marel GA; Codée JDC, Furanosyl Oxocarbenium Ion Conformational Energy Landscape Maps as a Tool to Study the Glycosylation Stereoselectivity of 2-Azidofuranoses, 2-Fluorofuranoses and Methyl Furanosyl Uronates. Chem. Eur. J 2019, 25, 7149–7157. [PubMed: 30882938]

(27). Bamhaoud T; Sanchez S; Prandi J 1,2,5-Ortho Esters of D-Arabinose as Versatile Arabinofuranosidic Building Blocks. Concise Synthesis of the Tetrasaccharidic Cap of the Lipoarabinomannan. Chem. Commun 2000, 659–660.

(28). Sanchez S; Bamhaoud T; Prandi J A Comprehensive Glycosylation System for the Elaboration of Oligoarabinofuranosides. Tetrahedron Lett. 2000, 41, 7447–7452.

(29). Ishiwata A; Munemura Y; Ito Y Nap Ether Mediated Intramolecular Aglycon Delivery: A Unified Strategy for 1,2-*cis*-Glycosylation. Eur. J. Org. Chem 2008, 4250–4263.

(30). Zhu X; Kawatkar S; Rao Y; Boons G-J Practical Approach for the Stereoselective Introduction of β-Arabinofuranosides. J. Am. Chem. Soc 2006, 128, 11948–11957. [PubMed: 16953636]

(31). Crich D; Pedersen CM; Bowers AA; Wink DJ On the Use of 3,5-*O*-Benzylidene and 3,5-*O*-(Di-*tert*-butylsilylene)-2-*O*-benzylarabinothiofuranosides and Their Sulfoxides as Glycosyl Donors for the Synthesis of β-Arabinofuranosides: Importance of the Activation Method. J. Org. Chem 2007, 72, 1553–1565. [PubMed: 17286432]

(32). Wang Y; Maguire-Boyle S; Dere RT; Zhu X Synthesis of β-D-Arabinofuranosides: Stereochemical Differentiation Between D- and L-Enantiomers. Carbohydr. Res 2008, 343, 3100–3106. [PubMed: 18809174]

(33). Imamura A; Lowary TL β-Selective Arabinofuranosylation Using a 2,3-*O*-Xylylene-Protected Donor. Org. Lett 2010, 12, 3686–3689. [PubMed: 20704416]

(34). Tilve MJ; Gallo-Rodriguez C Glycosylation Studies on Conformationally Restricted 3,5-*O*-(Di-*tert*-butylsilylene)-D-galactofuranosyl Trichloroacetimidate Donors for 1,2-*cis* α-D-Galactofuranosylation. Carbohydr. Res 2011, 346, 2838–2848. [PubMed: 22050997]

(35). Zhang L; Shen K; Taha HA; Lowary TL Stereocontrolled Synthesis of α-Xylofuranosides Using a Conformationally Restricted Donor. J. Org. Chem 2018, 83, 7659–7671. [PubMed: 29895148]

(36). Gadikota RR; Callam CS; Wagner T; Del Fraino B; Lowary TL 2,3-Anhydro Sugars in Glycoside Bond Synthesis. Highly Stereoselective Syntheses of Oligosaccharides Containing α- and β-Arabinofuranosyl Linkages. J. Am. Chem. Soc 2003, 125, 4155–4165. [PubMed: 12670238]

(37). Mukaiyama T; Suda S Diphosphonium Salts as Effective Reagents for Stereoselective Synthesis of 1,2-*cis*-Ribofuranosides. Chem. Lett 1990, 19, 1143–1146.

(38). Babu Mereyala H; Hotha S; Gurjar MK Synthesis of Pentaarabinofuranosyl Structure Motif a of Mycobacterium Tuberculosis. Chem. Commun 1998, 685–686.

(39). Désiré J; Prandi J Synthesis of Methyl β-D-Arabinofuranoside 5-[1D (and L)-*myo*-Inositol 1-Phosphate], the Capping Motif of the Lipoarabinomannan of Mycobacteriumsmegmatis. Carbohydr. Res 1999, 317, 110–118. [PubMed: 10466210]

(40). Subramaniam V; Lowary TL Synthesis of Oligosaccharide Fragments of Mannosylated Lipoarabinomannan from Mycobacterium Tuberculosis. Tetrahedron 1999, 55, 5965–5976.

(41). D'Souz FW; Lowary TL The First Total Synthesis of a Highly Branched Arabinofuranosyl Hexasaccharide Found at the Nonreducing Termini of Mycobacterial Arabinogalactan and Lipoarabinomannan. Org. Lett 2000, 2, 1493–1495. [PubMed: 10814481]

(42). Yin H; D'Souz FW; Lowary TL Arabinofuranosides from Mycobacteria: Synthesis of a Highly Branched Hexasaccharide and Related Fragments Containing β-Arabinofuranosyl Residues. J. Org. Chem 2002, 67, 892–903. [PubMed: 11856034]

(43). Lee YJ; Lee K; Jung EH; Jeon HB; Kim KS Acceptor-Dependent Stereoselective Glycosylation: 2'-CB Glycoside-Mediated Direct β-D-Arabinofuranosylation and Efficient Synthesis of the Octaarabinofuranoside in Mycobacterial Cell Wall. Org. Lett 2005, 7, 3263–3266. [PubMed: 16018636]

(44). Joe M; Sun D; Taha H; Completo GC; Croudace JE; Lammas DA; Besra GS; Lowary TL The 5-Deoxy-5-methylthio-xylofuranose Residue in Mycobacterial Lipoarabinomannan. Absolute Stereochemistry, Linkage Position, Conformation, and Immunomodulatory Activity. J. Am. Chem. Soc 2006, 128, 5059–5072. [PubMed: 16608340]

(45). Gola G; Tilve MJ; Gallo-Rodriguez C Influence of the Solvent in Low Temperature Glycosylations with *O*-(2,3,5,6-Tetra-*O*-benzyl-β-D-galactofuranosyl) Trichloroacetimidate for 1,2-*cis* α-D-Galactofuranosylation. Carbohydr. Res 2011, 346, 1495–1502. [PubMed: 21645887]

(46). Liu Q-W; Bin H-C; Yang J-S β-Arabinofuranosylation Using 5-*O*-(2-Quinolinecarbonyl) Substituted Ethyl Thioglycoside Donors. Org. Lett 2013, 15, 3974–3977. [PubMed: 23879464]

(47). Thadke SA; Mishra B; Hotha S Facile Synthesis of β- and α-Arabinofuranosides and Application to Cell Wall Motifs of M. Tuberculosis. Org. Lett 2013, 15, 2466–2469. [PubMed: 23659307]

(48). Abronina PI; Fedina KG; Podvalnyy NM; Zinin AI; Chizhov AO; Kondakov NN; Torgov VI; Kononov LO The Use of *O*-Trifluoroacetyl Protection and Profound Influence of the Nature of Glycosyl Acceptor in Benzyl-Free Arabinofuranosylation. Carbohydr. Res 2014, 396, 25–36. [PubMed: 25079596]

(49). Islam M; Gayatri G; Hotha S Influence of Steric Crowding on Diastereoselective Arabinofuranosylations. J. Org. Chem 2015, 80, 7937–7945. [PubMed: 26195010]

(50). Westheimer F Why Nature Chose Phosphates. Science 1987, 235, 1173–1178. [PubMed: 2434996]

(51). Weijers CAGM; Franssen MCR; Visser GM Glycosyltransferase-Catalyzed Synthesis of Bioactive Oligosaccharides. Biotechnol. Adv 2008, 26, 436–456. [PubMed: 18565714] For other examples of thiourea-catalyzed glycosylations see references 52-57:

(52). Balmond EI; Coe DM; Galan MC; McGarrigle EM, α-Selective Organocatalytic Synthesis of 2-Deoxygalactosides. Angew. Chem. Int. Ed 2012, 51, 9152–9155.

(53). Palo-Nieto C; Sau A; Williams R; Galan MC, Cooperative Brønsted Acid-Type Organocatalysis for the Stereoselective Synthesis of Deoxyglycosides. J. Org. Chem 2017, 82, 407–414. [PubMed: 28004941]

(54). Peng P; Schmidt RR, Acid–Base Catalysis in Glycosidations: A Nature Derived Alternative to the Generally Employed Methodology. Acc. Chem. Res 2017, 50, 1171–1183. [PubMed: 28440624]

(55). Williams R; Galan MC, Recent Advances in Organocatalytic Glycosylations. Eur. J. Org. Chem 2017, 6247–6264.

(56). Nielsen MM; Pedersen CM, Catalytic Glycosylations in Oligosaccharide Synthesis. Chem. Rev 2018, 118, 8285–8358. [PubMed: 29969248]

(57). Bradshaw GA; Colgan AC; Allen NP; Pongener I; Boland MB; Ortin Y; McGarrigle EM, Stereoselective Organocatalyzed Glycosylations – Thiouracil, Thioureas and Monothiophthalimide Act as Brønsted Acid Catalysts at Low Loadings. Chem. Sci 2019, 10,

508–514. [PubMed: 30713648] For other examples of organocatalyzed glycosylations see references 58-62:

(58). Kobayashi Y; Nakatsuji Y; Li S; Tsuzuki S; Takemoto Y, Direct *N*-Glycofunctionalization of Amides with Glycosyl Trichloroacetimidate by Thiourea/Halogen Bond Donor Co-Catalysis. Angew. Chem. Int. Ed 2018, 57, 3646–3650.

(59). Xu C; Loh CCJ, An Ultra-Low Thiourea Catalyzed Strain-Release Glycosylation and a Multicatalytic Diversification Strategy. Nat. Commun 2018, 9, 4057. [PubMed: 30282986]

(60). Levi SM; Jacobsen EN Catalyst-Controlled Glycosylations. Organic Reactions 2019, 100, 801–852.

(61). Xu C; Loh CCJ, A Multistage Halogen Bond Catalyzed Strain-Release Glycosylation Unravels New Hedgehog Signaling Inhibitors. J. Am. Chem. Soc 2019, 141, 5381–5391. [PubMed: 30848592]

(62). Ghosh T; Mukherji A; Kancharla PK, Open-Close Strategy toward the Organocatalytic Generation of 2-Deoxy-Ribosyl Oxocarbenium Ions: Pyrrolidine Salts Catalyzed Synthesis of 2-Deoxy-Ribofuranosides. Eur. J. Org. Chem 2019, 7488–7498.

(63). Levi SM; Li Q; Rötheli AR; Jacobsen EN Catalytic Activation of Glycosyl Phosphates for Stereoselective Coupling Reactions. Proc. Natl. Acad. Sci. USA 2019, 116, 35–39. [PubMed: 30559190]

(64). Palmacci ER; Plante OJ; Seeberger PH Oligosaccharide Synthesis in Solution and on Solid Support with Glycosyl Phosphates. Eur. J. Org. Chem 2002, 595–606.

(65). Hashimoto S-I; Honda T; Ikegami S A Rapid Efficient Synthesis of 1,2-*trans*-β-Linked Glycosides via Benzyl- or Benzoyl-protected Glycopyranosyl Phosphates. J. Chem. Soc., Chem. Commun 1989, 685–687.

(66). Sabesan S; Neira S Synthesis of Glycosyl Phosphates and Azides. Carbohydr. Res 1992, 223, 169–185.

(67). Illarionov PA; Torgov VI; Hancock IC; Shibaev V Synthesis of Glycosyl Phosphates from Acetylated Glycosyl Nitrates. Tetrahedron Lett. 1999, 40, 4247–4250.

(68). Tsuda T; Nakamura S; Hashimoto S A Highly Stereoselective Construction of 1,2-*trans*-β-glycosidic Linkages Capitalizing on 2-Azido-2-deoxy-D-glycosyl Diphenyl Phosphates as Glycosyl Donors. Tetrahedron 2004, 60, 10711–10737.

(69). Plante OJ; Andrade RB; Seeberger PH Synthesis and Use of Glycosyl Phosphates as Glycosyl Donors. Org. Lett 1999, 1, 211–214. [PubMed: 10905866]

(70). Garcia BA; Gin DY Synthesis of Glycosyl-1-phosphates via Dehydrative Glycosylation. Org. Lett 2000, 2, 2135–2138. [PubMed: 10891249]

(71). Plante OJ; Palmacci ER; Andrade RB; Seeberger PH Oligosaccharide Synthesis with Glycosyl Phosphate and Dithiophosphate Triesters as Glycosylating Agents. J. Am. Chem. Soc 2001, 123, 9545–9554. [PubMed: 11572674]

(72). Li Y; Singh G Synthesis of D-arabinofuranosides Using propane-1,3-diyl Phosphate as the Anomeric Leaving Group. Tetrahedron Lett. 2001, 42, 6615–6618.

(73). Plaza PGJ; Bhongade BA; Singh G Synthesis of Chiral Carbohydrate Ionic Liquids. Synlett 2008, 19, 2973–2976.

(74). Kennedy CR; Lehnherr D; Rajapaksa NS; Ford DD; Park Y; Jacobsen EN Mechanism-Guided Development of a Highly Active Bis-thiourea Catalyst for Anion-Abstraction Catalysis. J. Am. Chem. Soc 2016, 138, 13525–13528. [PubMed: 27704810]

(75). Park Y; Harper KC; Kuhl N; Kwan EE; Liu RY; Jacobsen EN Macrocyclic Bis-thioureas Catalyze Stereospecific Glycosylation Reactions. Science 2017, 355, 162–166. [PubMed: 28082586]

(76). Akiyama Y; Kato K Structure of Hydroxyproline-arabinoside from Tobacco Cells. Agric. Biol. Chem 1977, 41, 79–81.

(77). van Holst G-J; Varner JE Reinforced Polyproline II Conformation in a Hydroxyproline-Rich Cell Wall Glycoprotein from Carrot Root. Plant. Physiol 1984, 74, 247–251. [PubMed: 16663405]

(78). Finch P; Siriwardena AH Stereoselective *O*-Glycosylation of *trans*-4-Hydroxy-L-proline Derivatives Promoted by Silver Zeolite. Glyconj. J 1989, 6, 477–488.

(79). Showalter AM Structure and Function of Plant Cell Wall Proteins. Plant Cell 1993, 5, 9–23. [PubMed: 8439747]

(80). Kieliszewski MJ; Lamport DTA Extensin: Repetitive Motifs, Functional Sites, Post-translational Codes, and Phylogeny. Plant. J 1994, 5, 157–172. [PubMed: 8148875]

(81). Shpak E; Barbar E; Leykam JF; Kieliszewski MJ Contiguous Hydroxyproline Residues Direct Hydroxylproline Arabinosylation in *Nicotania tabacum*. J. Biol. Chem 2001, 276, 11272–11278. [PubMed: 11154705]

(82). Plante OJ; Palmacci ER; Andrade RB; Seeberger PH, Oligosaccharide Synthesis with Glycosyl Phosphate and Dithiophosphate Triesters as Glycosylating Agents. J. Am. Chem. Soc 2001, 123, 9545–9554. [PubMed: 11572674]

(83). Elshahawi SI; Shaaban KA; Kharel MA; Thorson JS A Comprehensive Review of Glycosylated Bacterial Natural Products. Chem. Soc. Rev 2015, 44, 7591–7697. [PubMed: 25735878]

(84). Qin X; Xie Y; Huang H; Chen Q; Ma J; Li Q; Ju J Enzymatic Synthesis of GDP-α-L-fucofuranose by MtdL and Hyg20. Org. Lett 2018, 20, 1015–1018. [PubMed: 29380608]

(85). Tefsen B; Ram AFJ; van Die I; Routier FH Galactofuranose in Eukaryotes: Aspects of Biosynthesis and Functional Impact. Glycobiol. 2012, 22, 456–469.

(86). Latge J-P Galactofuranose Containing Molecules in *Aspergillus fumigatus*. Med. Mycol 2009, 47, 104–109.

(87). Howell HG; Brodfuehrer PR; Brundidge SP; Benigni DA; Sapino C Jr. Antiviral Nucleosides. A Stereospecific, Total Synthesis of 2'-Fluoro-2'-deoxy-β-D-arabinofuranosyl Nucleosides. J. Org. Chem 1988, 53, 85–88.

(88). Santschi N; Gilmour R, Comparative Analysis of Fluorine-Directed Glycosylation Selectivity: Interrogating C2 [OH→F] Substitution in D-Glucose and D-Galactose. Eur. J. Org. Chem 2015, 6983–6987.

(89). Aiguabella N; Holland MC; Gilmour R, Fluorine-Directed 1,2-*trans* Glycosylation of Rare Sugars. Org. Biomol. Chem 2016, 14, 5534–5538. [PubMed: 26880180]

(90). Wang X; Woods RJ Insights into Furanose Solution Conformations: Beyond the Two-State Model. J. Biomol. NMR 2016, 64, 291–305. [PubMed: 26968894]

(91). Diemoz KM; Franz AK NMR Quantification of Hydrogen-Bond-Activating Effects for Organocatalysts Including Boronic Acids. J. Org. Chem 2019, 84, 1126–1138. [PubMed: 30516381]

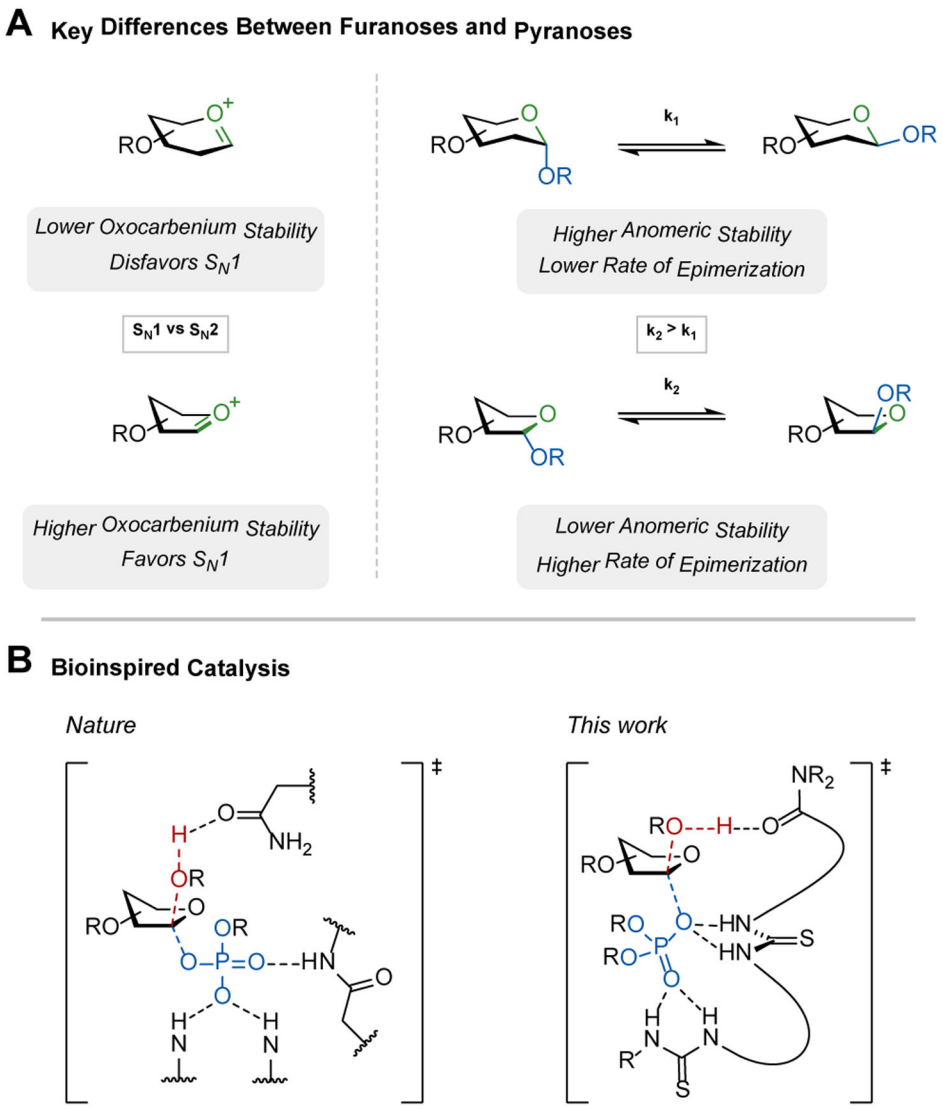

Figure 1.

A) Key differences between furanoses and pyranoses regarding reactivity at the anomeric position, and B) hydrogen-bond activation of anomeric phosphates in Nature vs. proposed hydrogen-bond activation using synthetic bis-thiourea catalysts.

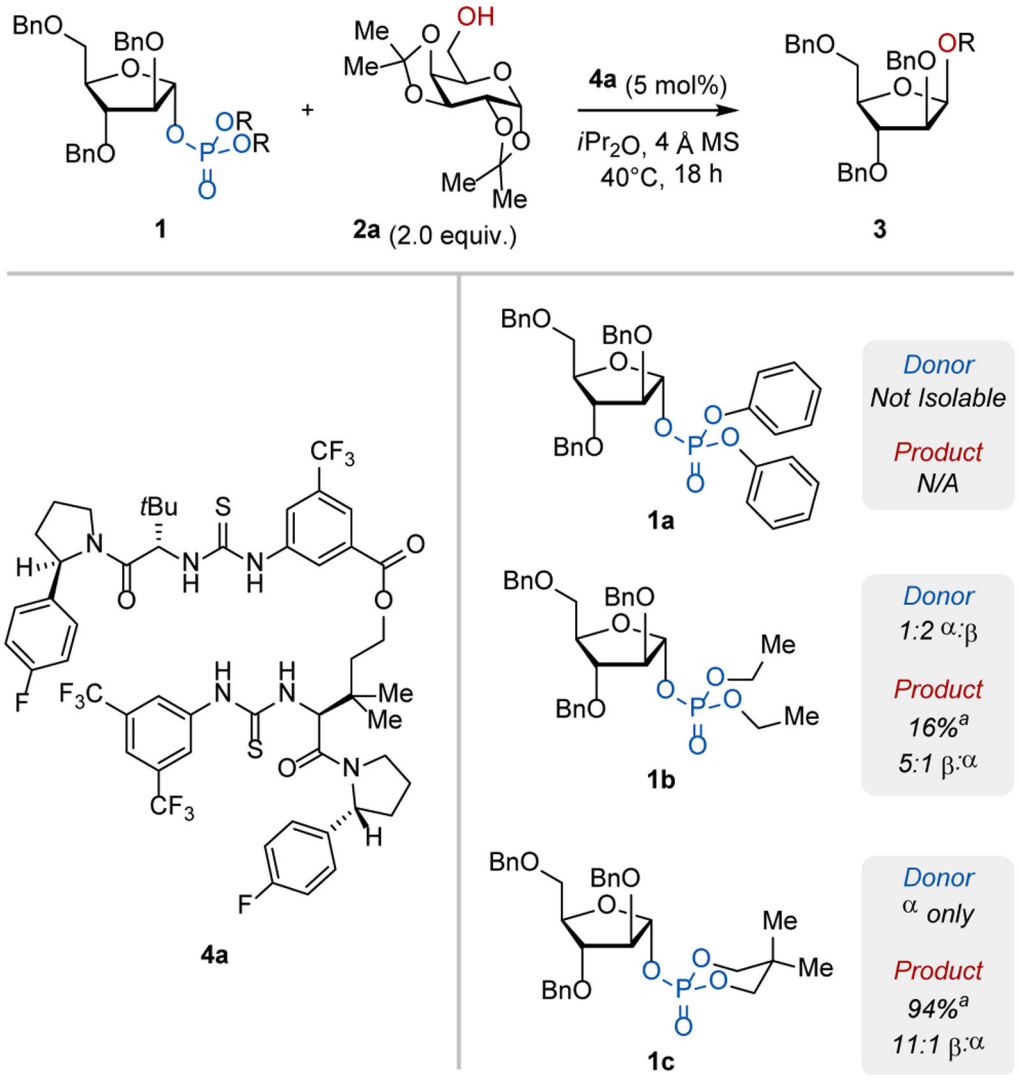

Figure 2.

Reaction optimization with respect to the identity of the anomeric phosphate leaving group

[a] Yield determined through ^{1}H NMR integration against an internal standard.

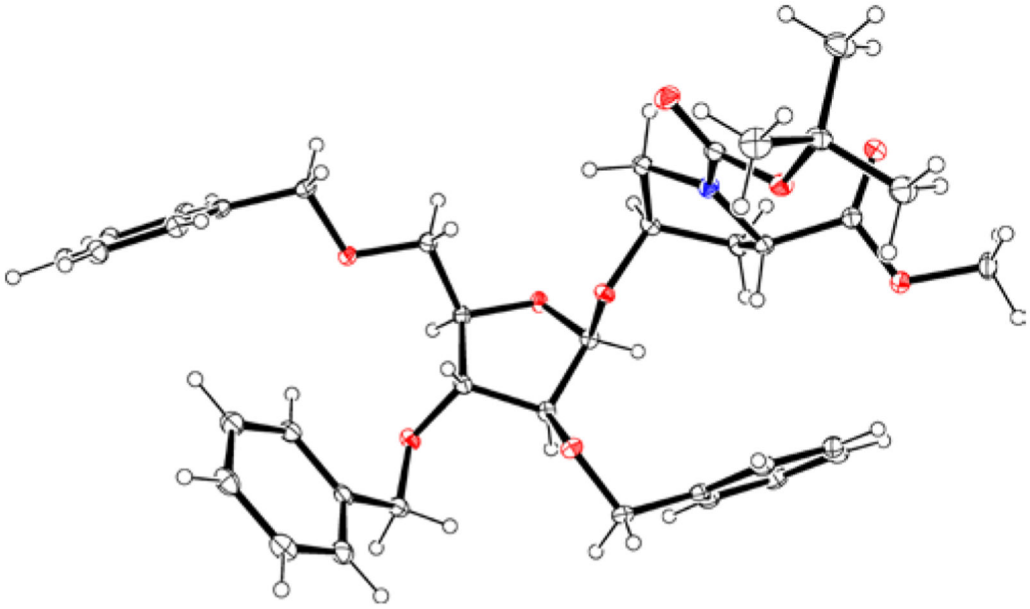

Figure 3.
X-Ray crystal structure of product **3r**. Thermal ellipsoids are shown at the 30% probability level.

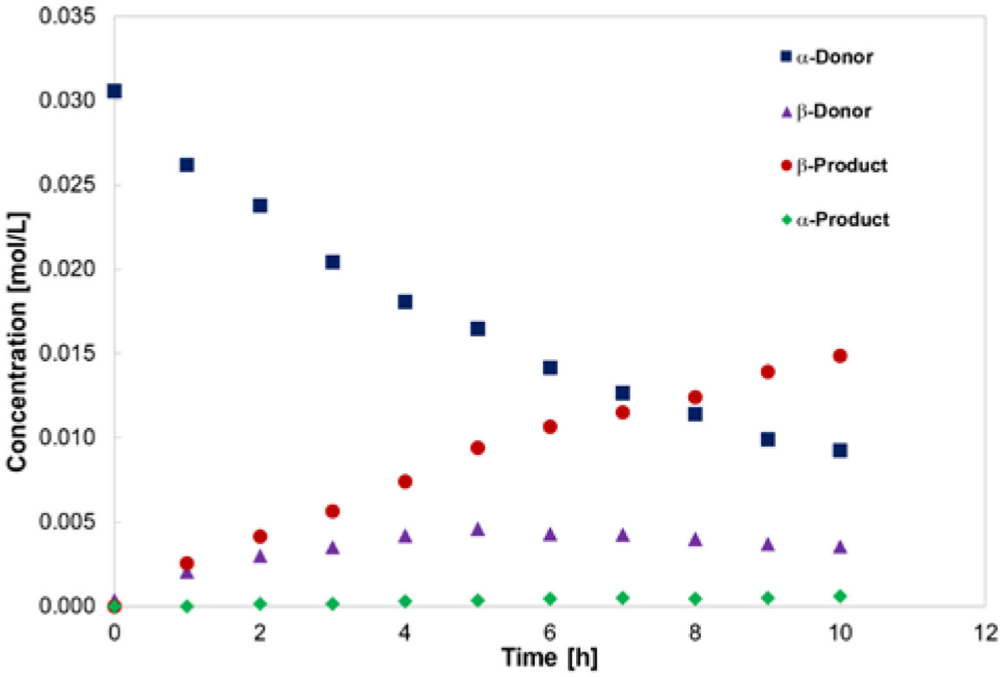

Figure 4.

Reaction progress analysis of the coupling of arabinose phosphate **1c** with *N*-Boc-L-threonine methyl ester **2b**.

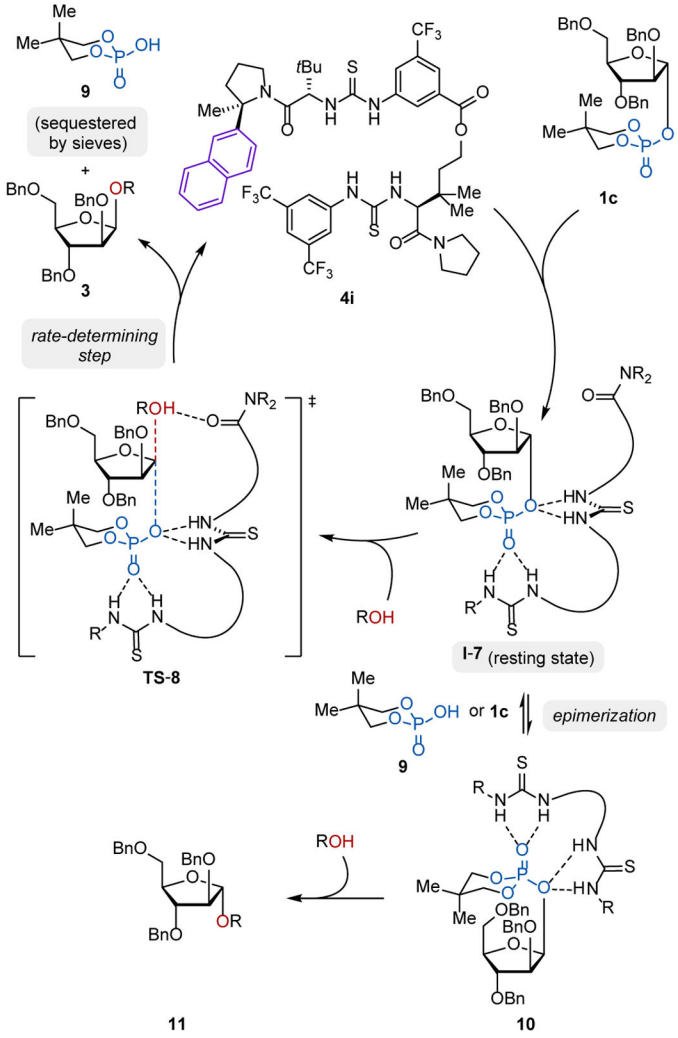

Scheme 1.
Proposed Catalytic Cycle.

J Am Chem Soc. Author manuscript; available in PMC 2021 February 26.

Table 1.

Initial Catalyst Optimization

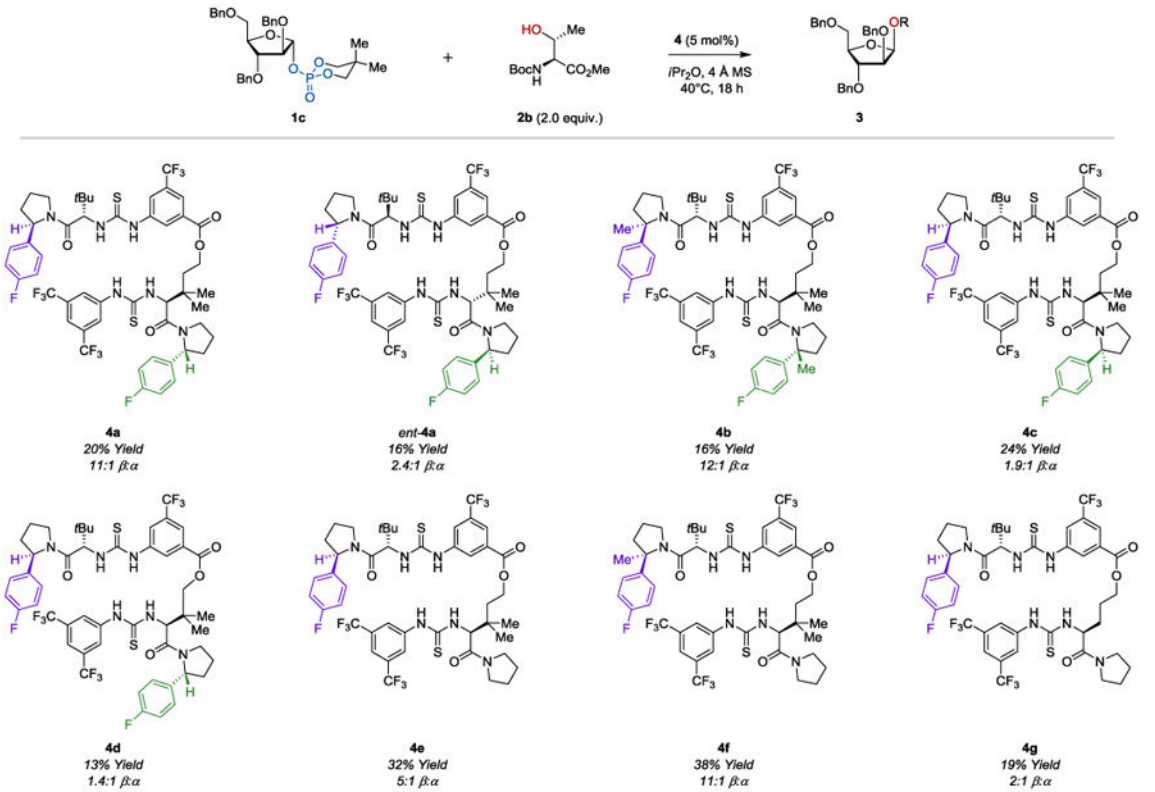

Standard reaction conditions: reactions were performed with arabinose phosphate **1c** (0.018 mmol, 1.0 equiv.), protected threonine **2b** (0.036 mmol, 2.0 equiv.), the specified catalyst (0.0009 mmol, 5 mol %), 1,3,5-trimethoxybenzene (0.018 mmol, 1.0 equiv.), 45 mg 4 Å molecular sieves in iPr$_2$O (0.45 mL). Yields and anomeric ratios were determined by ^{1}H NMR spectroscopy.

Table 2.

Optimization of Catalyst Aryl Substituent and Control Experiments

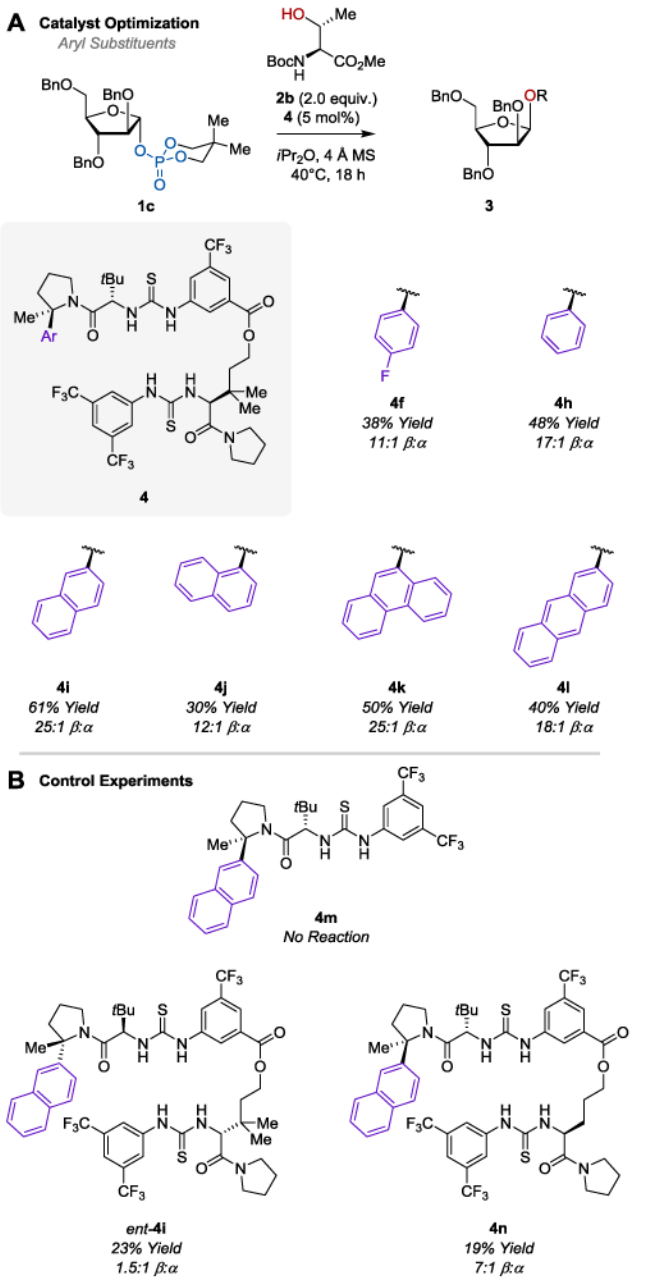

Standard reaction conditions: reactions were performed with arabinose phosphate **1c** (0.018 mmol, 1.0 equiv.), protected threonine **2b** (0.036 mmol, 2.0 equiv.), the specified catalyst (0.0009 mmol, 5 mol%), 1,3,5-trimethoxybenzene (0.018 mmol, 1.0 equiv.), 45 mg 4 Å molecular sieves in iPr$_2$O (0.45 mL). Product anomeric ratios were determined ^{1}H NMR spectroscopy. Yields and anomeric ratios were determined by ^{1}H NMR spectroscopy.

Table 3.

Acceptor Scope for the Arabinofuranose Phosphate Glycosylation

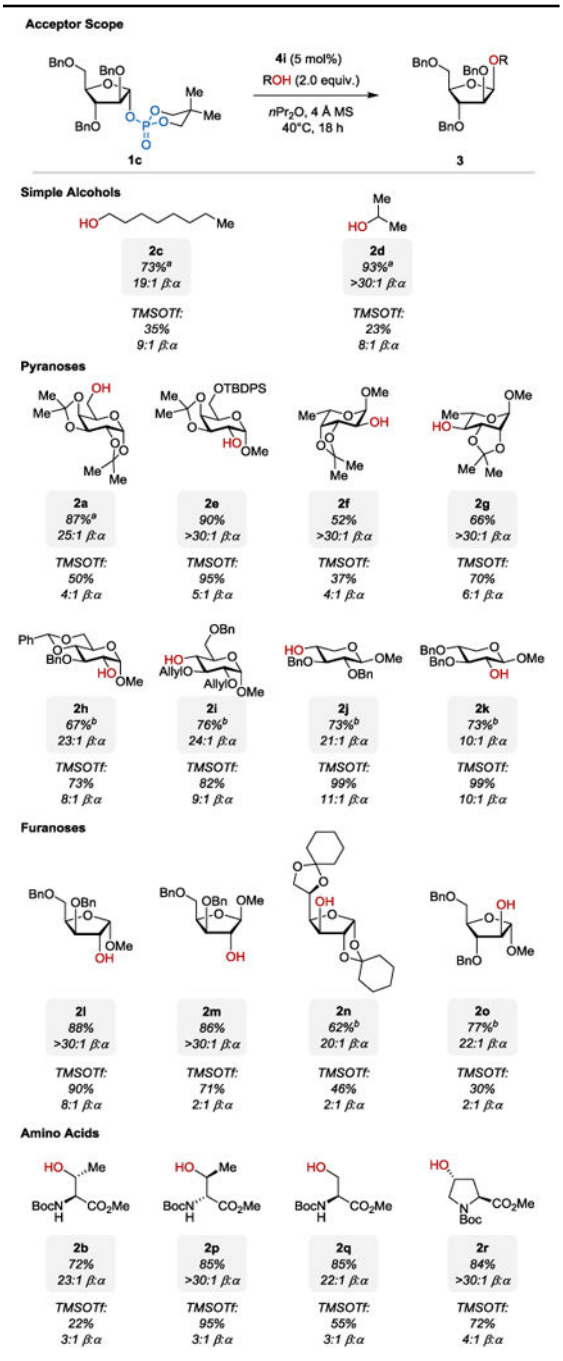

Standard reactions conditions: Reactions were performed with 0.2 mmol arabinose phosphate, 0.4 mmol acceptor in nPr$_2$O (5 mL) using 5 mol% catalyst and 500 mg 4 Å molecular sieves with constant stirring at 40 °C for 18 h. Product anomeric ratios were determined ^{1}H NMR spectroscopy. Yields given for the catalytic reaction are isolated yields, while yields for the TMSOTf reaction were determined by ^{1}H NMR spectroscopy. [a] Reaction time: 3 h. [b] Reaction time: 48 h.

Table 4.

Donor Scope and Stereochemical Permutations for the Furanose Phosphate Glycosylation.

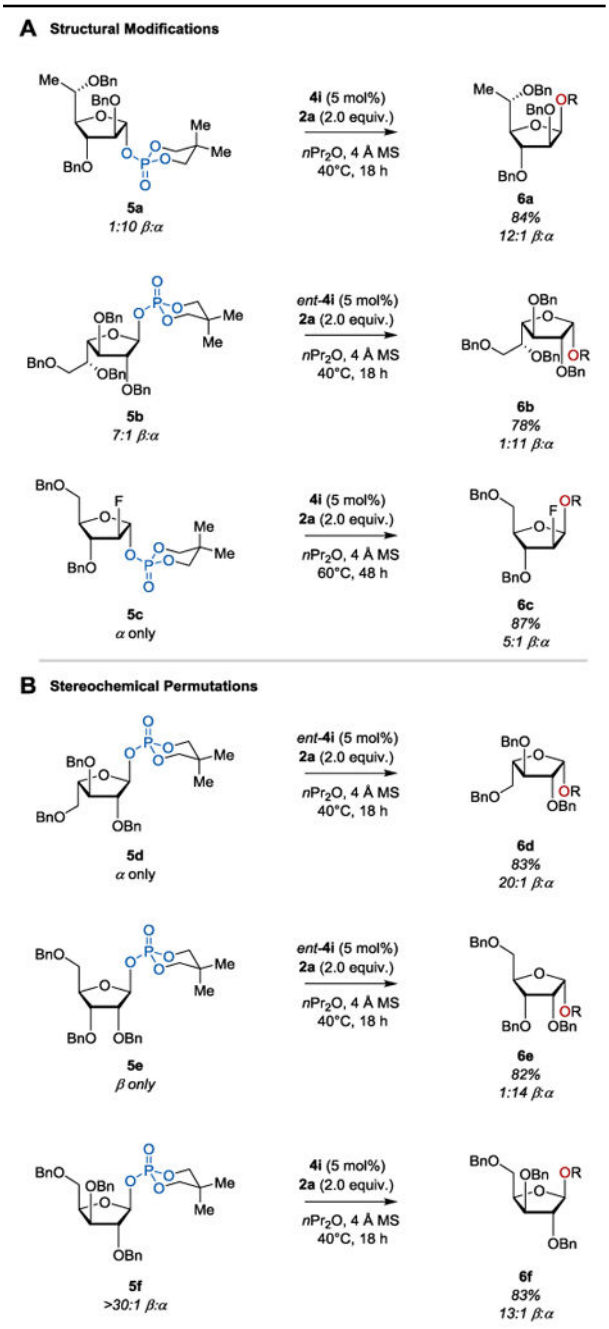

Standard reactions conditions: Reactions were performed with 0.2 mmol arabinose phosphate, 0.4 mmol acceptor in nPr$_2$O (5 mL) using 5 mol% catalyst loading and 500 mg 4 Å molecular sieves with constant stirring at 40 °C for 18 h. Yields given are isolated yields after purification. Yields and anomeric ratios were determined ^{1}H NMR spectroscopy.

Table 5.

Influence of Donor Anomeric Composition on the Selectivity of Furanose Glycosylation.

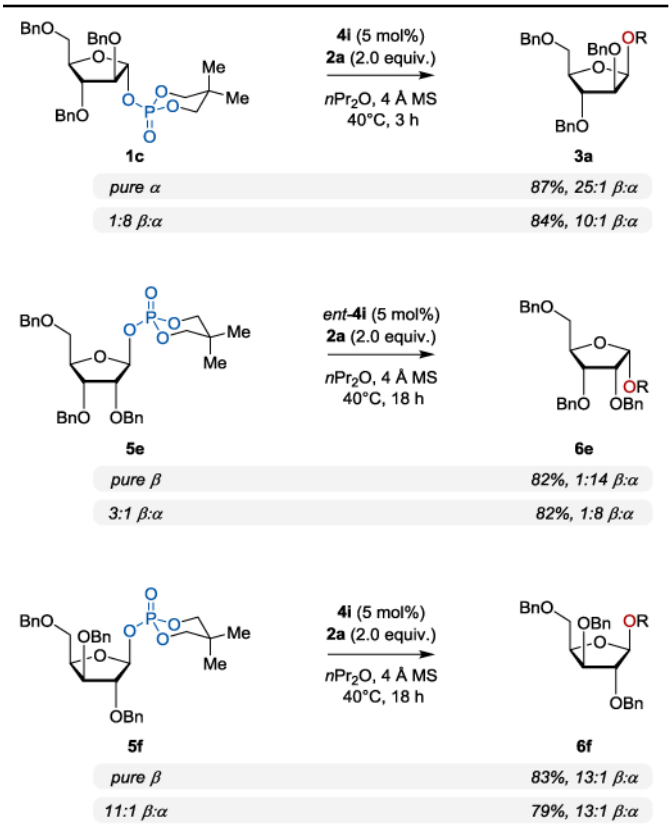

Standard reaction conditions: Reactions were performed with 0.2 mmol arabinose phosphate, 0.4 mmol acceptor in nPr$_2$O (5 mL) using 5 mol% catalyst loading and 500 mg 4 Å molecular sieves with constant stirring at 40 °C for 18 h. Yields given are isolated yields after purification. Yields and anomeric ratios were determined ^{1}H NMR spectroscopy.